HHS Public Access

Author manuscript

J Immunol. Author manuscript; available in PMC 2015 June 13.

Published in final edited form as:

J Immunol. 2008 December 15; 181(12): 8688–8699.

Lipoxin A_4 Counterregulates GM-CSF Signaling in Eosinophilic Granulocytes[1]

Vitaliy Starosta[*], **Konrad Pazdrak**[*], **Istvan Boldogh**[†], **Tetyana Svider**[‡], and **Alexander Kurosky**[2,*,‡]

[*]Department of Biochemistry and Molecular Biology, University of Texas Medical Branch, Galveston, TX 77555

[†]Department of Microbiology and Immunology, University of Texas Medical Branch, Galveston, TX 77555

[‡]National Heart, Lung, and Blood Institute Proteomics Center, University of Texas Medical Branch, Galveston, TX 77555

Abstract

Eosinophils are granulated leukocytes that are involved in many inflammation-associated pathologies including airway inflammation in asthma. Resolution of eosinophilic inflammation and return to homeostasis is in part due to endogenous chemical mediators, for example, lipoxins, resolvins, and protectins. Lipoxins are endogenous eicosanoids that demonstrate antiinflammatory activity and are synthesized locally at sites of inflammation. In view of the importance of lipoxins (LXs) in resolving inflammation, we investigated the molecular basis of LXA_4 action on eosinophilic granulocytes stimulated with GM-CSF employing the eosinophilic leukemia cell line EoL-1 as well as peripheral blood eosinophils. We report herein that LXA_4 (1–100 nM) decreased protein tyrosine phosphorylation in EoL-1 cells stimulated with GM-CSF. Additionally, the expression of a number of GM-CSF-induced cytokines was inhibited by LXA_4 in a dose-dependent manner. Furthermore, using a proteomics approach involving mass spectrometry and immunoblot analysis we identified 11 proteins that were tyrosine phosphorylated after GM-CSF stimulation and whose phosphorylation was significantly inhibited by LXA_4 pretreatment. Included among these 11 proteins were α-fodrin (non-erythroid spectrin) and actin. Microscopic imaging showed that treatment of EoL-1 cells or blood eosinophils with GM-CSF resulted in the reorganization of actin and the translocation of α-fodrin from the cytoplasm to the plasma membrane. Importantly, α-fodrin translocation was prevented by LXA_4 but actin reorganization was not. Thus, the mechanism of LXA_4 action likely involves prevention of activation of

[1]This study was supported by the National Institutes of Health National Heart, Lung, and Blood Institute's Proteomics Initiative N01-HV-28184 (to A.K.), National Institute for Environmental Health Sciences Center Grant P30-ES006676 (to J. Halpert),National Institute of Allergy and Infectious Diseases Grant P01 AI062885 (to A.Brasier) and a James W. McLaughlin postdoctoral fellowship grant to V. Starosta.

[2]Address correspondence and reprint requests to Dr. Alexander Kurosky, Department of Biochemistry and Molecular Biology, 301 University Boulevard, University of Texas Medical Branch, Galveston, TX 77555. akurosky@utmb.edu.

Disclosures: The authors have no financial conflicts of interest.

eosinophilic granulocytes by GM-CSF through inhibition of protein tyrosine phosphorylation and modification of some cytoskeletal components.

Lipoxins (LXs)[3] are endogenous eicosanoids that mediate antiinflammatory activity and are synthesized locally from arachidonate at sites of inflammation. LXA_4 and its isomer LXB_4 are the major lipoxins synthesized in mammals so far reported (see reviews in Refs. 1, 2). Two aspirin-induced lipoxins (15-epi-LXA_4 and 15-epi-LXB_4) are endogenous 15*R* enantiomers of LXA_4 and LXB_4 that demonstrate common bioreactivity with LXA_4 and LXB_4 but are more potent (1). LXA_4 is an especially important endogenous down-regulator of inflammation produced in many inflammation-associated pathologies including eosinophil-related pulmonary disorders (3, 4). The effectiveness of LXA_4 to counteract inflammation has been demonstrated in a number of cell culture and animal studies (5–7). Previous studies of allergic inflammation showed that LXA_4 and 15-epi-LXA_4 dramatically blocked allergic eosinophil airway influx while concurrently increasing circulating eosinophilia and inhibiting the early edema and neutrophilia associated with allergic reaction (4). These observed effects were distinct from leukotriene antagonism and potently blocked both allergic airway inflammation and hyperreactivity (8). Furthermore, LXA_4 and analogs significantly decreased allergen-induced eosinophilic pleurisy in sensitized rats (4). Lipoxin blockade of allergic eosinophilia was independent of mast cell degranulation and involved inhibition of IL-5, eotaxin, and platelet-activating factor (4). Potential mechanisms of LXA_4 action have been proposed (7, 9, 10) but taken together they do not adequately explain the multifaceted antiinflammatory molecular mechanism associated with LXA_4. Importantly, eosinophils are known to synthesize lipoxins. Eosinophil-enriched leukocytes from eosinophilic donors when challenged in vitro with the ionophore A23187 produced several lipoxygenase-derived compounds, including LXA_4 (11). Also, leukocytes can be primed by GM-CSF to produce lipoxins (12) and airway biosynthesis of LXA_4, and increased expression of its receptor can be induced by allergen challenge as well (13). Importantly, a high-affinity G protein-coupled receptor (ALX) for LXA_4 has been described for a number of cell types (2) and likely functions in eosinophils as indirectly indicated in murine studies (12). However, a direct molecular characterization of the ALX receptor in eosinophils has not been reported.

GM-CSF is a major survival and activating factor for hematopoietic cells that primes mature macrophages, eosinophils, and neutrophils and is known as a pleiotropic and proinflammatory cytokine (14). The respiratory epithelium expresses significant levels of GM-CSF, and infiltrating leukocytes can be induced to synthesize GM-CSF as an autocrine growth factor by inflammatory and chemotactic stimuli. GM-CSF can greatly enhance leukocyte oxidative burst activity and mediator release and serves as a major leukocyte survival factor in inflammatory lesions (15, 16). Adenoviral-mediated GM-CSF gene transfer in the lung induces lung eosinophilia, airway fibrosis, as well as marked macrophage accumulation (17). GM-CSF also primes sensitization to allergens and is directly implicated in the inflammatory responses of respiratory pollutants (18). GM-CSF is

[3]Abbreviations used in this paper: LX, lipoxin; 1DE, one-dimensional electrophoresis; 2DE, two-dimensional electrophoresis; GMRβ, GM-CSF β-chain receptor; IPG, immobilized pH gradient; LDS, lithium dodecyl sulfate; LXA_4, lipoxin A_4, 5*S*,6*R*,15*S*-trihydroxy-7,9,13-*trans*-11-*cis*-eicosatetraenoic acid; MS, mass spectrometry; RT, room temperature.

produced by both Th1 and Th2 cells and is responsible for promoting the differentiation of eosinophils from promyelocytes. Thus, since GM-CSF is produced by macrophages, eosinophils, and epithelial cells of asthmatic patients (19), the endogenous production of GM-CSF likely has an important role in the pathogenesis of allergic diseases and asthma and represents a putative target for therapeutic interventions by compounds like lipoxins.

In this study we have focused on the modulatory action of LXA_4 on GM-CSF-induced protein phosphorylation in eosinophilic cells and the resulting consequences on their activation. Using phosphoproteomic techniques, we found that LXA_4 significantly suppressed GM-CSF-induced phosphorylation of a number of proteins. Analysis of lipoxin-modified proteins by mass spectrometry and Western blotting identified several proteins critical for GM-CSF signaling pathways and cytoskeleton reorganization, including α-fodrin, a nonerythroid spectrin, and actin. Furthermore, we demonstrate that LXA_4 inhibits GM-CSF signaling in eosinophilic cells and prevents redistribution of some cytoskeletal elements (e.g., α-fodrin). Thus, we provide strong evidence that LXA_4 can effectively modulate protein phosphorylation involved in GM-CSF-induced cell activation of eosinophils and can affect cytoskeletal proteins. For much of this study we primarily used the EoL-1 cell model, a leukemia eosinophilic cell line first described by Saito et al. (20). This cell line provided several experimental advantages since human eosinophils comprise only a small percentage of peripheral leukocytes. Use of these cells has been reported in a number of studies (21, 22).

Materials and Methods

Cells and reagents

EoL-1 cells were obtained from the German Collection of Microorganisms and Cell Cultures. The cells were grown (10^6 cells/ml) in RPMI 1640 medium containing 10% (v/v) FBS, 100 U/ml penicillin, and 100 mg/ml streptomycin under a humidified atmosphere of 5% CO_2 and 95% air at 37°C. Cell culture media, FBS, and antibiotics (penicillin and streptomycin) were obtained from Invitrogen. Human peripheral blood eosinophils were isolated and purified as we previously described (23). FITC-phalloidin was a product of Sigma-Aldrich. Primary and FITC- and rhodamine-conjugated secondary Abs were obtained from Santa Cruz Biotechnology. Human recombinant GM-CSF was from PeproTech. LXA_4 was purchased from the Cayman Chemical. The reagent was aliquoted and stored at −80°C until use.

EoL-1 cell treatments

Typically EoL-1 cells were incubated for 16 h in serum-free medium to decrease basal protein phosphorylation and then pretreated with 1–100 nM LXA_4 for 30 min at 37°C. For protein phosphorylation studies, cells were stimulated with 10 ng/ml GM-CSF for 10 min.

Two-dimensional electrophoresis (2DE)/lithium dodecyl sulfate (LDS)-PAGE

After GM-CSF stimulation (10 ng/ml) for 10 min, with and without LXA_4 pretreatment (50 nM, 30 min, 37°C), EoL-1 cells (25×10^6) were harvested by centrifugation at $300 \times g$ for 10 min at 4°C, washed twice with ice-cold PBS, and lysed on ice in cell lysis buffer

consisting of 50 mM Tris-HCl (pH 7.4), 150 mM NaCl, 1.0% (v/v) Triton X-100, 1.0 mM EDTA, 1.0 mM PMSF, 1 mg/ml aprotinin, 1 mg/ml leupeptin, 1 mg/ml pepstatin, 1.0 mM Na_3VO_4, and 1.0 mM NaF. After incubation for 60 min on ice, samples were centrifuged at 14,000 × *g* for 10 min at 4°C. Supernatants were desalted before 2DE/LDS-PAGE using a protein extraction kit (EMD Biosciences). After precipitation, protein samples were collected by centrifugation (14,000 × *g*, 10 min, 4°C), briefly dried by vacuum centrifugation, and then redissolved in 150 μl of rehydration buffer (7 M urea, 2 M thiourea, 2% CHAPS, 1% DTT, 2% pH 4–7 ampholytes) containing protease inhibitors (Roche Diagnostics). Protein quantification was performed using the Bio-Rad Bradford protein assay kit. The protein samples (150 μg for 7-cm strips) in rehydration buffer were directly applied to immobilized pH gradient (IPG) strips (pH 4–7, Amersham Biosciences). Isoelectric focusing was conducted using an IPGphor apparatus (Amersham Biosciences) at 20°C with the following protocol: 50 V for 11 h (active rehydration), 250 V gradient for 1 h, 500 V gradient for 1 h, 1000 V for 1 h, 4000 V gradient for 2 h, and held at 4000 V for 11 h. Following focusing, the IPG strips were equilibrated with a reducing solution of 50 mM Tris-HCl (pH 8.8) containing 6 M urea, 2% SDS, 30% glycerol, and 1% DTT. Following reduction, the strips were reacted with 5% iodoacetamide in the above Tris-HCl buffer without DTT for 10 min. The reduced and alkylated strips were stored at −80°C until use or loaded directly onto 12–16% polyacrylamide gels.

Gel staining and analysis

After 2DE/LDS-PAGE gels were fixed in 7% acetic acid and 10% methanol for 1 h and then stained overnight with Sypro Ruby fluorescent protein gel stain (Bio-Rad). After destaining, the gels were scanned with a Fuji FLA-5100 imager (Fujifilm Medical Systems USA) using a 532-nm excitation source and a 575-nm emission filter. For the detection of phosphoproteins, the gels were stained using Pro-Q Diamond phosphoprotein gel stain (Invitrogen) according to the manufacturer's protocol. Additionally, duplicate gels were electroblotted onto polyvinylidene difluoride membranes and stained with mouse anti-pTyr mAb (clone PY100; Cell Signaling Technology) (see “Western immunoblot analysis” below).

Image analysis of 2DE gel phosphoprotein spot patterns

Protein expression patterns associated with enhanced phosphorylation after GM-CSF stimulation that was inhibited by LXA_4 pretreatment were evaluated for significant differences (>2-fold) by image analysis using Progenesis SameSpots software version 2.0 (Nonlinear USA). Three gel replicates were analyzed with proteins representative of three separate experiments. The Progenesis software was also used to compare the Sypro Ruby-stained gels with the anti-pTyr-stained gels (separate gels). Anti-pTyr-stained phosphoprotein spots that changed after LXA_4 treatment were identified on the Sypro Ruby-stained gels and were subsequently excised and analyzed by mass spectrometry (MS).

Protein identification by MS

After staining with Sypro Ruby, UV-visible protein spots were excised and subjected to protein identification after trypsin digestion. Mass spectra of peptide digests were obtained

using a model 4800 MALDI-TOF-TOF MS (Applied Biosystems). Proteins were identified using the Swiss-Prot database and the Mascot algorithm. Positive protein identifications were accepted for those with expectation values of 1×10^{-3} or smaller as we previously reported (24). Expectation values were derived from Mascot scores (see www.matrixscience.com).

Western immunoblot analysis

Separated proteins in a LDS-polyacrylamide gel were electroblotted onto a polyvinylidene difluoride membrane for 1 h using the XCell SureLock Novex Mini-Cell system (Invitrogen) (20). Before probing with Abs, the blotted membranes were blocked with 3% (w/v) BSA in 1% TBS-Tween 20 for 1 h. For the detection of phosphorylated tyrosine residues, the membranes were probed with mouse anti-pTyr mAb clone PY100. After washing 3× with TBS-Tween 20 at room temperature (RT), the membranes were incubated for 1 h with a HRP-conjugated secondary Ab. Membranes were washed three times in TBS-Tween 20 and developed with ECL reagent (Millipore).

Immunoprecipitation

Cells (25×10^6) were preincubated with 50 nM LXA_4 for 30 min and stimulated with 10 ng/ml GM-CSF for 10 min before washing with ice-cold PBS (pH 7.4) and lysis. After removal of cell debris by centrifugation at 14,000 × *g* for 20 min, lysates were pretreated for 1 h with protein G-agarose beads (Pierce) and then incubated with 3 μg of polyclonal Ab for 2 h followed by 1 h of incubation with protein G-agarose beads. Abs used for immunoprecipitation were anti-fodrin and anti-GM-CSF β-chain receptor (GMRβ), and anti-SHP-1 and anti-SHP-2 were used for Western blotting (Santa Cruz Biotechnology). Immunoprecipitates were washed three times with lysis buffer and heated in LDS sample buffer for 5 min (95°C). Coimmunoprecipitation of GMRβ was performed similarly using anti-GMRβ except that the immunoprecipitates were washed five times with PBS.

α-Fodrin isolation and analysis

Cell cytoskeleton proteins containing α-fodrin were evaluated essentially according to the method of Watts and Howard (25) using Triton X-100 detergent. Cells (5×10^6) were suspended in 1% Triton X-100 for 30 min at 4°C. A Triton-insoluble, low-speed pellet fraction representing the crude membrane cytoskeleton was isolated by sedimentation of cell lysates at 14,000 × *g* for 20 min. The supernatant containing the detergent-soluble fraction representing the cellular actin cytoskeleton was then examined for α-fodrin content by one-dimensional Western blot analysis.

Tyrosine phosphatase analysis

The tyrosine phosphatase assay was performed with EoL-1 cells stimulated with GM-CSF, with or without LXA_4 pretreatment, using a commercially available kit (Tyrosine Phosphatase Assay System; Promega) for total cellular protein tyrosine phosphatase activity and a *p*-nitrophenyl phosphate assay for the measurement of phosphotyrosine phosphatase activity of SHP-1 and SHP-2 after immunoprecipitation. Briefly, cells (25×10^6) were harvested in a phosphatase buffer (50 nM Tris-HCl (pH 7.0) containing 1 mM EDTA,

0.05% 2-ME, and 1% Triton X-100) and included one tablet of a protease inhibitor mixture (Roche Diagnostics) per 10 ml of buffer and centrifuged at 12,000 rpm for 5 min at 4°C. Endogenous phosphate in the supernatants was removed using Sephadex G-25 spin columns. The sample flow through was then incubated with 100 μM tyrosine phosphopeptide substrate (in kit) for 10 min at 30°C, followed by incubation with molybdate dye solution. Tyrosine phosphatase analyses were representative of three separate experiments.

Fluorescence microscopy

EoL-1 cells or human peripheral blood eosinophils (10^5), treated with GM-CSF, LXA_4, or both together, were cytospun to coverslips. Microscopic imaging was performed essentially as we previously reported (26). Briefly, after treatment, cells were washed, air dried, and fixed for 10 min with 4% paraformaldehyde in PBS (pH 7.4) and permeabilized. The cells were then incubated for 60 min at 37°C with either anti-α-fodrin or anti-actin (1–19) (Santa Cruz Biotechnology) diluted 1/200 in PBS-Tween 20. After being washed three times for 15 min each time with PBS-Tween 20, the cells were incubated for 1 h at RT with FITC-conjugated secondary Ab (Santa Cruz Biotechnology) diluted 1/200 in PBS-Tween 20. For FITC-phalloidin staining, cell preparations were incubated for 15 min at RT. Nuclei of cells were stained for 15 min with DAPI (4′,6-diamidino-2-phenylindole; 10 ng/ml; excitation 345 nm, emission 455 nm; Molecular Probes). The cells were then mounted in antifade medium (Dako) on a microscope slide and the fluorescent images were photographed. Confocal microscopy was performed on a Zeiss LSM510 META system, and images were captured at ×60 to ×192 magnification.

F-actin organization analysis by flow cytometry

Actin organization was analyzed using flow cytometry. EoL-1 cells (1×10^7/ml, 1 ml) suspended in RPMI 1640 medium were stimulated with GM-CSF (10 ng/ml) for 10 min at 37°C with or without LXA_4 pretreatment. Subsequently, cells were fixed with 4% paraformaldehyde for 30 min at RT and permeabilized with 1% Triton X-100 for 15 min. Cells were then incubated with FITC-phalloidin (100 ng/ml) in the dark for 15 min at RT, washed with PBS, resuspended in PBS containing 0.5% paraformaldehyde, and analyzed by flow cytometry with a FACSCanto analyzer (BD Biosciences) using CellQuest analysis software. The relative F-actin content expressed as FITC-phalloidin fluorescence intensity of the various treatments employed was compared with control resting cells that received no treatment. The FACS analysis results are representative of three repeats.

Results

LXA_4 homogeneity

Since LXA_4 is generally known to be unstable, we evaluated the homogeneity of the Cayman Chemical product that we used by negative ion mode electrospray ionization-MS (Waters/Micromass QTOF2) and by RP-HPLC. HPLC showed only a single peak, as shown in Fig. 1A, and electrospray ionization-MS gave the expected authentic product peak with m/z 351.5 (Fig. 1B). We concluded that the LXA_4 used in our studies was authentic and reasonably homogeneous. These analyses paralleled earlier documentation of the physical

properties of LXA_4 that used RP-HPLC and gas chromatography-MS after derivatization (27).

Evaluation of protein tyrosine phosphorylation by 2DE gels

Using serum-starved EoL-1 cells we assessed protein tyrosine phosphorylation in whole-cell lysates after 10 min of stimulation with GM-CSF (10 ng/ml) in combination with pretreatment of cells with 50 nM LXA_4 for 30 min. Subsequently, 2DE gels were electroblotted and stained with anti-pTyr. Blotted images revealed significantly more protein phosphorylation after GM-CSF stimulation, which was considerably inhibited by LXA_4 pretreatment (Fig. 2A). Duplicate gels run in parallel (GM-CSF and GM-CSF + LXA_4, Fig. 2A) were stained with Sypro Ruby and revealed equal protein loading (results not shown). The Progenesis software was able to match a number of phosphorylated protein spots revealed by anti-pTyr staining on two-dimensional Western blots with Sypro Ruby-stained spots on two-dimensional gels. Protein spots whose phosphorylation was increased by GM-CSF and then decreased by LXA_4 pretreatment were excised and submitted for peptide mass analysis for protein identification. MS results showing 10 identified proteins are given in Table I. Their positions on a 2DE gel are shown by arrows in Fig. 2B. Western blot analysis of proteins of interest validated the 2DE/MS results (see below).

One-dimensional electrophoresis (1DE) gel analysis of GM-CSF induced protein tyrosine phosphorylation inhibited by LXA_4

Pretreatment of starved EoL-1 cells with increasing concentrations of LXA_4 for 30 min resulted in the reduction of protein tyrosine phosphorylation of a number of proteins induced by GM-CSF as assessed by 1DE anti-pTyr Western blot analysis of whole-cell lysates (Fig. 3A). Fig. 3B is a repeat of Fig. 3A but at a lower protein loading to better visualize the more intensely stained bands. Notably, some protein bands did not show any changes and thereby gave evidence of equal protein loading. The most effective concentration of LXA_4 that inhibited GM-CSF-induced protein tyrosine phosphorylation under the given experimental conditions was observed in the range of 50–100 nM. It is noteworthy, however, that LXA_4 itself induced some protein phosphorylation when added alone, and this effect was concentration-dependent. Fig. 3C is the same gel as shown in Fig. 3A but stripped and reacted with anti-actin. It confirmed the position of actin bands as well as equal protein loading.

Effect of LXA_4 on the phosphorylation of ERK1/2 and SHP-2 after GM-CSF stimulation

Both ERK1/2 and SHP-2 are known to acquire increased phosphorylation after GM-CSF treatment of human eosinophils and play important roles in signal transduction (23). Thus, we investigated whether LXA_4 had any effect on their level of phosphorylation. As shown in Fig. 4, for whole-cell lysates from cells pretreated with increasing LXA_4 concentrations followed by GM-CSF (10 ng/ml) treatment, the phosphorylation of ERK1/2 and SHP-2 was influenced differentially by LXA_4. LXA_4 pretreatment inhibited GM-CSF-mediated ERK1/2 phosphorylation in a dose-dependent manner. On the other hand, the phosphorylation of SHP-2 was not affected by LXA_4 alone but was further synergistically increased to a plateau level with the combined effect of GM-CSF and increasing concentrations of LXA_4.

Effect of LXA_4 on GM-CSF-induced phosphorylation and intracellular distribution of α-fodrin

Using 2DE (Fig. 2B and Table I) we observed an increase in the tyrosine phosphorylation of α-fodrin (nonerythoid α-spectrin) in EoL-1 cells treated with GM-CSF that was inhibited by LXA_4. Fodrin had not been investigated in eosinophils before, and in other cell types the phosphorylation of α-fodrin was reported to have appreciable functional importance (28, 29). Thus, we further investigated α-fodrin phosphorylation and cellular localization in EoL-1 cells after GM-CSF stimulation. Results of 1DE stained gels of anti-fodrin immunoprecipitates after treatment with GM-CSF with and without LXA_4 pretreatment are shown in Fig. 5. The gel in Fig. 5A, *left panel*, shows increased phosphorylation of α-fodrin after GM-CSF stimulation (Fig. 5A, *lane 2*) that was decreased by the addition of LXA_4 (Fig. 5A, *lane 3*), validating our 2DE results (Fig. 2A). Fig. 5A, *right panel*, shows equal protein loading after staining with Sypro Ruby. Fig. 5B shows the relative ratios of the gel fluorescence intensities representing normalized α-fodrin phosphorylation. Translocation of fodrin from the cytoplasm to cell membranes was observed after treatment with GM-CSF, and this translocation was prevented by LXA_4 pretreatment. Fig. 5C shows the result of Western blot analysis using anti-α-fodrin immunostaining of Triton-soluble (cytoplasmic) and Tritoninsoluble (plasma membrane) fractions of EoL-1 cells representing the cytoplasmic/membrane distribution of α-fodrin and the effect of GM-CSF and LXA_4 on this distribution.

Fluorescence microscopy

Since fodrin is a known actin-associated protein, we further examined the effects of GM-CSF and LXA_4 treatment on the cytoskeleton by microscopy using anti-fodrin and F-actin FITC-phalloidin to visualize F-actin. Fig. 6A clearly demonstrates the translocation of fodrin from the cytoplasm to the cell membrane after GM-CSF treatment. This translocation was prevented by pretreatment with LXA_4, further validating our results shown in the Western blot of Fig. 5C. The experiment was repeated with human peripheral blood eosinophils, and the same results were obtained as shown in Fig. 6A. Further evidence of cytoskeletal rearrangement after GM-CSF treatment is given in Fig. 6B in which the polymerized F-actin-specific FITC-phalloidin stain was employed. GM-CSF treatment of EoL-1 cells resulted in a dramatic rearrangement of F-actin that was not restored by pretreatment with LXA_4 (Fig. 6B). LXA_4 alone had no effect on F-actin. FACS analysis showed a 33% decrease in F-actin fluorescence intensity mediated by FITC-phalloidin in GM-CSF-treated samples (Fig. 6C). That the reduction in fluorescence was not prevented by LXA_4 was consistent with fluorescence microscopy results shown in Fig. 6B. Taken together, these results strongly suggested at least partial depolymerization of F-actin by GM-CSF.

Protein tyrosine phosphatase activity after LXA_4 treatment

Next, we determined total protein tyrosine phosphatase activity of samples treated with either GM-CSF, LXA_4 alone, or both GM-CSF and LXA_4 in combination. As shown in Fig. 7A, LXA_4 treatment alone increased total protein tyrosine phosphatase activity by 2-fold when compared with the control. Interestingly, GM-CSF treatment also increased tyrosine phosphatase activity as did the combined treatment of LXA_4 and GM-CSF (Fig. 7A).

Additionally, two protein tyrosine phosphatases (SHP-1 and SHP-2) that participate in GM-CSF signal transduction were also investigated. A completely different pattern of activity was demonstrated by SHP-1 phosphatase (Fig. 7B, *upper panel*) when compared with SHP-2 (Fig. 7B, *lower panel*) after GM-CSF stimulation. LXA_4 alone showed some increase of SHP-1 activity and decreased GM-CSF stimulated SHP-1 phosphatase activity when used in combination. On the other hand, SHP-2 activity was hardly influenced by LXA_4 alone but showed a significant dose-dependent increase when used in combination with GM-CSF. It has been shown that receptor-mediated signaling is modulated by complex events including the action of phosphatases (30). Fig. 7C is a Western blot analysis of GMRβ immunoprecipitates after combinations of LXA_4 and GM-CSF treatments with the immunoreagents shown. Again, the immunoprecipitation pattern of SHP-1 and SHP-2 was different. SHP-1 phosphatase was elevated only in samples treated with LXA_4, demonstrating the translocation of SHP-1 to the GMRβ induced by LXA_4. SHP-2, on the other hand, was associated with GMRβ only after GM-CSF stimulation and it significantly increased in combination with LXA_4, consistent with results shown in Fig. 4.

Inflammatory cytokine profiling after LXA_4 treatment

We also evaluated cytokine profiles before and after pretreatment of GM-CSF-stimulated EoL-1 cells with LXA_4. As listed above, a panel of 25 human cytokines was investigated using Luminex-type beads and Bio-Rad Laboratories' Bio-Plex multiplex instrumentation. Of the 25 cytokines, the levels of 8 were significantly changed by GM-CSF treatment, including IL-2R, IL-6, IL-8, IL-10, IL-13, RANTES, MCP-1, and eotaxin. Three of these 8 cytokines (IL-8, IL-13, and eotaxin) were significantly decreased by pretreatment of EoL-1 cells with LXA_4 (Fig. 8).

Discussion

We have attempted to define the molecular basis of the antiinflammatory action of LXA_4 in association with GM-CSF since GM-CSF is one of the crucial cytokines affecting eosinophil function in asthma and allergy (19). Clearly, and importantly, we have shown that LXA_4 is considerably inhibitory to GM-CSF action. Inhibition of GM-CSF eosinophil activation by LXA_4 would, at least in part, explain its antiinflammatory action. In activated eosinophils, leukotrienes, cytokines, reactive oxygen, and nitrogen species, eosinophil cationic protein and peroxidase are all increased and are thought to inflict much of the damage to the asthmatic airway epithelium and submucosa (31). In this report, we show that LXA_4 in a concentration-dependent manner can block tyrosine phosphorylation of proteins in EoL-1 cells stimulated with GM-CSF. The proteins involved in the LXA_4 inhibitory action included some of the key signaling molecules of the GM-CSF pathway, such as ERK1/2 and SHP-2. Additionally, the secretion of some cytokines was also inhibited, including IL-8, IL-13, and eotaxin. We also provided evidence that inhibition of activation of eosinophilic cells by LXA_4 was concomitant with suppression of phosphorylation of proteins involved in cytoskeletal organization, specifically fodrin and actin. The latter effect may be associated with increased activity of specific protein tyrosine phosphatases, for example, SHP-2 (Figs. 4 and 7B). Thus, we have provided new potential mechanisms of action for lipoxins that may explain some of the physiological effects of this important lipid mediator.

The priming and stimulatory actions of GM-CSF on eosinophils were reported previously to be associated with increased intracellular protein tyrosine phosphorylation (32). Although there is insufficient information about the action of LXA_4 on protein phosphorylation in various disease models, there is evidence that LXA_4 can block phosphorylation of leukocyte-specific protein 1 and alters phosphorylation and activation of components of the p38-MAPK cascade in chemoattractant-stimulated human neutrophils (6). Inhibition of ERK phosphorylation by LXA_4 may be one of the key events leading to the inhibition of inflammatory cytokine production in eosinophils (33). Our observations are in line with studies of fibroblasts and T cells where it was shown that ERK activation is attenuated in the presence of lipoxins (34). A correlation between LXA_4 action and increased SHP-2 phosphatase activity was shown in studies involving the inhibition of platelet-derived growth factor β receptor signaling (9); however, the role of this tyrosine phosphatase is still unclear (30). In general, LXA_4 seems to have an immunomodulatory property that returns the kinase/phosphatase balance of inflammation-altered tissues back to a steady-state and participates in the resolution of inflammation-related phenomena. Current thinking underscores a process involving switching of lipid mediator profiles from proinflammatory to antiinflammatory (e.g., leukotriene to lipoxin biosynthesis) (5).

Our investigation of tyrosine phosphorylation revealed 10 proteins that were phosphorylated after GM-CSF stimulation, and their phosphorylation was inhibited by LXA_4 pretreatment. Some proteins (e.g., glucosidase II α-subunit and ezrin) demonstrated multiple horizontal spots, suggesting additional posttranslational modifications. The biological significance of tyrosine phosphorylation of these proteins related mostly to their participation in cytoskeletal reorganization, cellular stress responses, oxidative stress, and cytoprotection (Table I). However, these proteins represented only a small proportion of high-abundance proteins that are typically seen on 2DE gels of a whole-cell proteome, and changes in the lesser abundant proteins were not assessed and require more extensive investigations.

Western blot analysis of GM-CSF- and LXA_4-treated cells using anti-pTyr Ab and anti-actin visualization showed a number of protein tyrosine phosphorylated bands that diminished with LXA_4 pretreatment. Two protein bands were especially notable (~42 and 21 kDa) that reacted with both anti-pTyr and anti-actin Ab. Increasing concentrations of LXA_4 reduced the level of observed anti-pTyr reactivity in both of these two protein bands. It is well known that actin can be cleaved in two, which accounted for the minor 21-kDa band. The observed 42-kDa band was consistent with the molecular mass of G-actin monomers. The doublet appearance of these bands may be due to differential phosphorylation. Actin phosphorylation on tyrosine has not been reported for eosinophils, although several laboratories have reported tyrosine phosphorylation of actin in other cells (35, 36). Proteome analysis identified α-actin to be one of the most abundant proteins in eosinophils (A. Kurosky, unpublished results).

Fodrin, an actin-binding protein and a nonerythroid spectrin homolog, is a heterodimer of α-chains (αI or αII) and β-chains (βI to βV) encoded by two and five genes, respectively, in mammals (28). In addition to actin, it possesses binding sites for calmodulin, Ca^{2+}, CD45, and possibly members of the phospholipid-binding annexin family of proteins. A number of functions have been described for fodrin, including membrane protein sorting, organization

of receptor domains, vesicular trafficking, endocytosis, and neurite outgrowth (37). Phosphorylation of serine on the β-chain of fodrin (38) and tyrosine on the α-chain (28) have been reported. Tyrosine phosphorylation of residue Y1176 of the αII-chain was shown in RCCD1 cells and transfected COS cells (28). It has been proposed that Y1176 phosphorylation inhibits the proteolysis of fodrin by calpain and thus plays a critical role in membrane-cytoskeleton interactions (28). These studies are in agreement with previous work showing rapid reorganization of fodrin with fragmentation of fodrin aggregates and concomitant translocation from the cytoplasm to the plasma membrane during lymphocyte activation (29). Our report herein is the first implicating the involvement of fodrin in eosinophil activation.

The first definable event in granulocytes activation is the transition from nonactivated to primed cellular state, which markedly enhances the functional response of cells to secondary stimulation (39). The organizational patterns of fodrin and CD45 were reported in primed and unprimed neutrophils and lymphocytes showing the relative depletion and enhancement of these proteins in the surface structure of resting and activated cells, respectively (40, 41). Thus, the activation-induced redistribution of cortical fodrin and reorganization of actin may be important steps in the priming of eosinophils after GM-CSF stimulation. We showed that both α-fodrin and actin were tyrosine phosphorylated after GM-CSF stimulation and that this phosphorylation was prevented by LXA_4 pretreatment. Moreover, the phosphorylation of α-fodrin after GM-CSF stimulation was concomitant with its translocation to the membrane. Our results were comparable with those of Lee et al. (29), who reported that lymphocytes have reserves of cytoplasmic fodrin, which can relocate to the plasma membrane following activation of the cell.

Further studies were conducted to inquire about fodrin and F-actin localization and organization after GM-CSF stimulation using immunofluorescence microscopy. Since EoL-1 cells are quite small with large nuclei, we also included peripheral blood eosinophils for further confirmation in these studies. As shown in Fig. 6, GM-CSF stimulation of either EoL-1 cells or blood eosinophils resulted in the translocation of α-fodrin to the plasma membrane. FACS analysis indicated substantial depolymerization of F-actin after GM-CSF stimulation that was not prevented by LXA_4 treatment (Fig. 6C). Furthermore, fluorescence microscopy using FITC-phalloidin showed considerable actin rearrangement after GM-CSF treatment that also was not prevented by LXA_4 treatment (Fig. 6B). These results gave strong evidence to support complex cytoskeletal involvement in the activation of eosinophils by GM-CSF and for the dysregulation of this process by LXA_4 Our results were consistent with the occurrence of α-fodrin modification(s) as a result of LXA_4 action that did not allow its association with the plasma membrane. Fodrin has also been reported to localize in nuclei of cells functioning in DNA synthesis and gene expression (42). Our immunofluorescence studies were unable to identify any occurrence of α-fodrin in nuclei of eosinophils under our experimental conditions. It is also possible that in the nucleus of eosinophils α-fodrin is complexed to other macromolecules such that immunoreactivity with the employed Ab was prevented.

Several studies have also implicated the involvement of actin organization in activated eosinophils and neutrophils. Boehme et al. (43) reported that eotaxin-stimulated eosinophils

activated p42/p44 MAPK, leading to changes in intracellular actin organization and polymerization. Kutsuna et al. (44) demonstrated that GM-CSF activation of neutrophils caused F-actin depolymerization similar to our observations with EoL-1 cells. LXA_4 can also regulate macrophage phagocytosis through facilitative actin cytoskeleton rearrangement and cell polarization (45). Reville et al. showed that LXA_4 stimulates the phosphorylation of key polarity organization molecules, namely, Akt, protein kinase Cζ, and glycogen synthase kinase-3β, and caused dephosphorylation of MYH9, a nonmuscle myosin H chain II isoform A, which is involved in cytoskeleton rearrangement (45). These results further underscore the involvement of LXA_4 in signal transduction and cytoskeleton rearrangement. Moreover, lipoxins have been shown to modulate the action of vascular endothelial growth factor in angiogenesis (46). A lipoxin analog inhibited endothelial cell migration by inhibiting actin polymerization and proper assembly of focal adhesions (46). Significant also are the results from in vitro and in vivo experiments that LXA_4 and analogs inhibited TNF-α-stimulated superoxide anion generation and IL-1β release by neutrophils and inhibited TNF-α-stimulated leukocyte trafficking in murine air pouches (47).

Tyrosine phosphorylation is a recognized key mechanism for signal transduction and the regulation of a broad spectrum of physiological processes. Receptor signaling is modulated by complex and highly regulated mechanisms that involve protein tyrosine kinases, protein tyrosine phosphatases, lipid phosphatases, ubiquitin ligases, and inhibitory adaptor molecules (30). In light of the central role played by protein tyrosine phosphorylation in immunoreceptor signaling, inhibition or prevention of this event may provide an effective method of interfering with cell activation (48). Our results showed that LXA_4 can increase total protein tyrosine phosphatase activity in the cell. However, the integral phosphatase activity observed does not represent the complex spatiotemporal distribution of each particular phosphatase studied. We found that protein tyrosine phosphatase SHP-1, which largely plays an inhibitory role in cellular signaling, was stimulated by LXA_4 alone and reached even higher levels of activity after GM-CSF stimulation, likely representing a reciprocal feedback mechanism that protects the cell from excessive activation. Concomitant treatment with both agents resulted in SHP-1 activity comparable with that elicited by LXA_4 alone, suggesting that LXA_4 abolished initial GM-CSF stimulatory signal with inhibition of consequent compensatory increase of feedback protein tyrosine phosphatase activity. Importantly, SHP-1 binding to GMRβ occurred only with LXA_4-treated samples. This may reflect the potentially pleiotropic inhibitory mechanism of LXA_4 action and warrants further investigation with other proinflammatory receptors. SHP-2 phosphatase activity, which plays an important role in signal transduction (34), increased significantly with combined LXA_4 and GM-CSF treatment. The importance of this observation is currently open-ended and requires further research. It is known that SHP-2 regulates the reorganization of the actin cytoskeleton through the RhoA- and Vav2-dependent signaling pathways in other tissues and might be instrumental in tissue remodeling (49).

The action of LXA_4 also demonstrated some features that are somewhat of a paradox. Addition of LXA_4 alone also increased phosphorylation of actin and ERK1/2 while in the same experiment GM-CSF-induced phosphorylation of actin and ERK1/2 were inhibited by LXA_4 A possible explanation for this apparent paradox is that under our experimental

conditions LXA_4 differentially induced specific phoshatases that effected target proteins and thereby enhanced intrinsic kinase activity. Alternatively, specific kinases for these proteins may have been up-regulated. Since lipoxins are not typically present in normal cellular conditions, the action of LXA_4 in naive cells may be different than in cells treated with GM-CSF plus LXA_4. More investigations are required and are planned to understand this phenomenon. The possibility that the observed increase in phosphorylation of some cellular proteins competitively inhibited GM-CSF protein phosphorylation, thus preventing eosinophil activation, is unlikely. First, 2DE Western blotted gels from LXA_4 treatment alone more closely resembled control untreated gels when compared with gels of cells treated with GM-CSF, which showed significantly more tyrosine phosphorylated proteins. Second, in preliminary experiments (results not shown) treatment of eosinophils with LXA_4 alone did not increase the expression of CD69, a recognized marker of eosinophils activation. Moreover, LXA_4 inhibited the up-regulation of CD69 by GM-CSF, further confirming the likely role of GM-CSF in preventing eosinophil activation.

It was previously reported that LXA_4 and aspirin-triggered lipoxin analogs attenuated the nuclear accumulation of AP-1 and NF-κB in both polymorphonuclear and mononuclear leukocytes and inhibited IL-8 mRNA expression and IL-8 release by 50% in response to LPS (7). Nanomolar concentrations of LXA_4 inhibited the IL-8 released by PBMC from patients with asthma (3). In this study we showed that the pretreatment of cells with LXA_4 resulted not only in the inhibition of protein tyrosine phosphorylation after 10 min of GM-CSF stimulation but also significantly decreased synthesis of proinflammatory cytokines after 24 h of coincubation with GM-CSF. Particularly interesting was the observation of the essentially complete inhibition of IL-8 secretion from EoL-1 cells, which increased 8-fold after GM-CSF stimulation. This may prove important in the treatment of severe asthma where an excess of GM-CSF and IL-8 in bronchoalveolar lavage was accompanied by increased numbers of eosinophils and neutrophils and a reduction in the amount of LXA_4 (3, 50).

In conclusion, we report herein that LXA_4, a naturally synthesized eicosanoid, can contribute to the active resolution of inflammation by inhibition of the complex and highly regulated molecular signaling that leads to eosinophil activation. LXA_4 appears to have the capability of dysregulating eosinophil activation signaling, likely by inhibiting protein tyrosine phosphorylation and modification of critical cytoskeletal proteins during GM-CSF activation.

Acknowledgments

We thank Drs. Anthony Haag and Robert English of the Mass Spectrometry Core of the University of Texas Medical Branch Biomolecular Resource Facility for mass spectrometry analysis and Dr. Zheng Wu for HPLC analysis. The technical assistance of Susan Stafford was much appreciated.

References

1. Serhan CN. Resolution phase of inflammation: novel endogenous antiinflammatory and proresolving lipid mediators and pathways. Annu Rev Immunol. 2007; 25:101–137. [PubMed: 17090225]

2. McMahon B, Mitchell S, Brady HR, Godson C. Lipoxins: revelations on resolution. Trends Pharmacol Sci. 2001; 22:391–395. [PubMed: 11478982]

3. Bonnans C, Vachier I, Chavis C, Godard P, Bousquet J, Chanez P. Lipoxins are potential endogenous antiinflammatory mediators in asthma. Am J Respir Crit Care Med. 2002; 165:1531–1535. [PubMed: 12045128]

4. Bandeira-Melo C, Bozza PT, Diaz BL, Cordeiro RS, Jose PJ, Martins MA, Serhan CN. Cutting edge: lipoxin (LX) A_4 and aspirin-triggered 15-epi-LXA_4 block allergen-induced eosinophil trafficking. J Immunol. 2000; 164:2267–2271. [PubMed: 10679058]

5. Levy BD, Clish CB, Schmidt B, Gronert K, Serhan CN. Lipid mediator class switching during acute inflammation: signals in resolution. Nat Immunol. 2001; 2:612–619. [PubMed: 11429545]

6. Ohira T, Bannenberg G, Arita M, Takahashi M, Ge Q, Van Dyke TE, Stahl GL, Serhan CN, Badwey JA. A stable aspirin-triggered lipoxin A_4 analog blocks phosphorylation of leukocyte-specific protein 1 in human neutrophils. J Immunol. 2004; 173:2091–2098. [PubMed: 15265945]

7. Jozsef L, Zouki C, Petasis NA, Serhan CN, Filep JG. Lipoxin A_4 and aspirin-triggered 15-epi-lipoxin A_4 inhibit peroxynitrite formation, NF-κB and AP-1 activation, and IL-8 gene expression in human leukocytes. Proc Natl Acad Sci USA. 2002; 99:13266–13271. [PubMed: 12235371]

8. Levy BD, Lukacs NW, Berlin AA, Schmidt B, Guilford WJ, Serhan CN, Parkinson JF. Lipoxin A_4 stable analogs reduce allergic airway responses via mechanisms distinct from CysLT1 receptor antagonism. FASEB J. 2007; 21:3877–3884. [PubMed: 17625069]

9. Mitchell D, O'Meara SJ, Gaffney A, Crean JK, Kinsella BT, Godson C. The Lipoxin A_4 receptor is coupled to SHP-2 activation: implications for regulation of receptor tyrosine kinases. J Biol Chem. 2007; 282:15606–15618. [PubMed: 17403678]

10. Machado FS, Johndrow JE, Esper L, Dias A, Bafica A, Serhan CN, Aliberti J. Anti-inflammatory actions of lipoxin A_4 and aspirin-triggered lipoxin are SOCS-2 dependent. Nat Med. 2006; 12:330–334. [PubMed: 16415877]

11. Serhan CN, Hirsch U, Palmblad J, Samuelson B. Formation of lipoxin A by granulocytes from eosinophilic donors. FEBS Lett. 1987; 217:242–246. [PubMed: 3109942]

12. Fiore S, Serhan CN. Formation of lipoxin and leukotrienes during receptor-mediated interactions of human platelets and recombinant human granulocyte/macrophage colony-stimulating factor-primed neutrophils. J Exp Med. 1990; 172:1451–1457. [PubMed: 2172436]

13. Levy BD, De Sanctis GT, Devchand PR, Kim E, Ackerman K, Schmidt BA, Szczeklik W, Drazem JM, Serhan CN. Multipronged inhibition of airway hyper-responsiveness and inflammation by lipoxin A_4. Nat Med. 2002; 8:1018–1023. [PubMed: 12172542]

14. Tai PC, Spry CJ. The effects of recombinant granulocyte-macrophage colony stimulating factor (GM-CSF) and interleukin-3 on the secretory capacity of human blood eosinophils. Clin Exp Immunol. 1990; 80:426–434. [PubMed: 2197048]

15. Hamilton JA. GM-CSF in inflammation and autoimmunity. Trends Immunol. 2002; 23:403–408. [PubMed: 12133803]

16. Fleetwood AJ, Cook AD, Hamilton JA. Functions of granulocyte macrophage colony-stimulating factor. Crit Rev Immunol. 2005; 25:405–428. [PubMed: 16167889]

17. Xing Z, Ohkawara Y, Jordana M, Graham F, Gauldie J. Transfer of granulocyte-macrophage colony-stimulating factor gene to rat lung induces eosinophilia, monocytosis, and fibrotic reactions. J Clin Invest. 1996; 97:1102–1110. [PubMed: 8613534]

18. Stampfli MR, Wiley RE, Neigh GS, Gajewska BU, Lei XF, Snider DP, Xing Z, Jordana M. GM-CSF transgene expression in the airway allows aerosolized ovalbumin to induce allergic sensitization in mice. J Clin Invest. 1998; 102:1704–1714. [PubMed: 9802884]

19. Robinson DS, Hamid Q, Ying S, Tsicopoulos A, Barkans J, Bentley AM, Corrigan C, Durham SR, Kay AB. Predominant TH2-like bronchoalveolar T-lymphocyte population in atopic asthma. N Engl J Med. 1992; 326:298–304. [PubMed: 1530827]

20. Saito H, Bourinbaiar A, Ginsburg M, Minato K, Ceresi E, Yamada K, Machover D, Breard J, Mathe G. Establishment and characterization of a new human eosinophilic leukemia cell line. Blood. 1985; 66:1233–1240. [PubMed: 2415185]

21. Wong CK, Ho CY, Lam CW, Zhang JP, Hjelm NM. Differentiation of a human eosinophilic leukemic cell line, EoL-1: characterization by the expression of cytokine receptors, adhesion

molecules, CD95 and eosinophilic cationic protein (ECP). Immunol Lett. 1999; 68:317–323. [PubMed: 10424438]

22. Griffin JH, Leung J, Bruner RJ, Caligiuri MA, Briesewitz R. Discovery of a fusion kinase in EOL-1 cells and idiopathic hypereosinophilic syndrome. Proc Natl Acad Sci USA. 2003; 100:7830–7835. [PubMed: 12808148]
23. Pazdrak K, Young TW, Stafford S, Olszewska-Pazdrak B, Straub C, Starosta V, Brasier A, Kurosky A. Cross-talk between ICAM-1 and GM-CSF receptor signaling modulates eosinophil survival and activation. J Immunol. 2008; 180:4182–4190. [PubMed: 18322230]
24. Forbus J, Spratt H, Wiktorowicz J, Wu Z, Boldogh I, Denner L, Kurosky A, Brasier RC, Luxon B, Brasier AR. Functional analysis of the nuclear proteome of human A549 alveolar epithelial cells by HPLC-high resolution 2-D gel electrophoresis. Proteomics. 2006; 6:2656–2672. [PubMed: 16586437]
25. Watts RG, Howard TH. Role of tropomyosin, alpha-actinin, and actin binding protein 280 in stabilizing Triton insoluble F-actin in basal and chemotactic factor activated neutrophils. Cell Motil Cytoskeleton. 1994; 28:155–164. [PubMed: 8087874]
26. Brasier AR, Spratt H, Wu Z, Boldogh I, Zhang Y, Garafolo RP, Casola A, Pashmi J, Haag A, Luxon B, Kurosky A. Nuclear heat shock response and novel nuclear domain 10 reorganization in respiratory syncytial virus-infected A549 cells identified by high-resolution two-dimensional gel electrophoresis. J Virol. 2004; 78:11461–11476. [PubMed: 15479789]
27. Serhan CN, Nicolaou KC, Webber SE, Veale CA, Drahlen SE, Pustinen TJ, Samuelson B. Lipoxin A stereochemistry and biosynthesis. J Biol Chem. 1986; 261:16340–16345. [PubMed: 3097008]
28. Nicolas G, Fournier CM, Galand C, Malbert-Colas L, Bournier O, Kroviarski Y, Bourgeois M, Camonis JH, Dhermy D, Grandchamp B, Lecomte MC. Tyrosine phosphorylation regulates alpha II spectrin cleavage by calpain. Mol Cell Biol. 2002; 22:3527–3536. [PubMed: 11971983]
29. Lee JK, Black JD, Repasky EA, Kubo RT, Bankert RB. Activation induces a rapid reorganization of spectrin in lymphocytes. Cell. 1988; 55:807–816. [PubMed: 3142688]
30. Pao LI, Badour K, Siminovitch KA, Neel BG. Nonreceptor protein-tyrosine phosphatases in immune cell signaling. Annu Rev Immunol. 2007; 25:473–523. [PubMed: 17291189]
31. Gleich GJ. Mechanisms of eosinophil-associated inflammation. J Allergy Clin Immunol. 2000; 105:651–663. [PubMed: 10756213]
32. Yousefi S, Green DR, Blaser K, Simon HU. Protein-tyrosine phosphorylation regulates apoptosis in human eosinophils and neutrophils. Proc Natl Acad Sci USA. 1994; 91:10868–10872. [PubMed: 7526384]
33. Bozinovski S, Jones JE, Vlahos R, Hamilton JA, Anderson GP. Granulocyte/macrophage-colony-stimulating factor (GM-CSF) regulates lung innate immunity to lipopolysaccharide through Akt/Erk activation of NF-κB and AP-1 in vivo. J Biol Chem. 2002; 277:42808–42814. [PubMed: 12208854]
34. Ariel A, Chiang N, Arita M, Petasis NA, Serhan CN. Aspirin-triggered lipoxin A_4 and B_4 analogs block extracellular signal-regulated kinase-dependent TNF-α secretion from human T cells. J Immunol. 2003; 170:6266–6272. [PubMed: 12794159]
35. Liu X, Shu S, Hong MS, Levine RL, Korn ED. Phosphorylation of actin Tyr-53 inhibits filament nucleation and elongation and destabilizes filaments. Proc Natl Acad Sci USA. 2006; 103:13694–13699. [PubMed: 16945900]
36. Rush J, Moritz A, Lee KA, Guo A, Goss VL, Spek EJ, Zhang H, Zha XM, Polakiewicz RD, Comb MJ. Immunoaffinity profiling of tyrosine phosphorylation in cancer cells. Nat Biotechnol. 2005; 23:94–101. [PubMed: 15592455]
37. Ohbayashi K, Fukura H, Inoue HK, Komiya Y, Igarashi M. Stimulation of L-type Ca^{2+} channel in growth cones activates two independent signaling pathways. J Neurosci Res. 1998; 51:682–696. [PubMed: 9545083]
38. Fowler VM, Adam EJ. Spectrin redistributes to the cytosol and is phosphorylated during mitosis in cultured cells. J Cell Biol. 1992; 119:1559–1572. [PubMed: 1469048]
39. Condliffe AM, Kitchen E, Chilvers ER. Neutrophil priming: pathophysiological consequences and underlying mechanisms. Clin Sci Lond. 1998; 94:461–471. [PubMed: 9682667]

40. Pradhan D, Morrow J. The spectrin-ankyrin skeleton controls CD45 surface display and interleukin-2 production. Immunity. 2002; 17:303–315. [PubMed: 12354383]

41. Stie J, Jesaitis AJ. Reorganization of the human neutrophil plasma membrane is associated with functional priming: implications for neutrophil preparations. J Leukocyte Biol. 2007; 81:672–685. [PubMed: 17170075]

42. McMahon LW, Walsh CE, Lambert MW. Human α-spectrim II and the Fanconi anemia proteins FANCA and FANCC interact to form a nuclear complex. J Biol Chem. 1999; 274:32904–32908. [PubMed: 10551855]

43. Boehme SA, Sullivan SK, Crowe PD, Santos M, Conlon PJ, Sriramarao P, Bacon KB. Activation of mitogen-activated protein kinase regulates eotaxin-induced eosinophil migration. J Immunol. 1999; 163:1611–1618. [PubMed: 10415066]

44. Kutsuna H, Suzuki K, Kamata N, Kato T, Hato F, Mizuno K, Kobayashi H, Ishii M, Kitagawa S. Actin reorganization and morphological changes in human neutrophils stimulated by TNF, GM-CSF, and G-CSF: the role of MAP kinases. Am J Physiol Cell Physiol. 2004; 286:C55–C64. [PubMed: 12954601]

45. Reville K, Crean JK, Vivers S, Dransfield I, Godson C. Lipoxin A_4 redistributes myosin IIA and Cdc42 in macrophages: implications for phagocytosis of apoptotic leukocytes. J Immunol. 2006; 176:1878–1888. [PubMed: 16424219]

46. Cezar-de-Mello PFT, Nascimento-Silva V, Villela GG, Fierro IM. Asprin-triggered lipoxin A_4 inhibition of VEGF-induced endothelial cell migration involves actin polymerization and focal adhesion assembly. Oncogene. 2006; 25:122–129. [PubMed: 16132039]

47. Hachicha M, Pouliot M, Petasis NA, Serhan CN. Lipoxin (LX) A_4 and asprin-triggered 15-epi-LXA_4 inhibit tumor necrosis factor 1α-initiated neutrophil responses and trafficking: regulators of a cytokine-chemokine axis. J Exp Med. 1999; 189:1923–1930. [PubMed: 10377187]

48. Veillette A, Latour S, Davidson D. Negative regulation of immunoreceptor signaling. Annu Rev Immunol. 2002; 20:669–707. [PubMed: 11861615]

49. Fernstrom K, Farmer P, Ali MS. Cytoskeletal remodeling in vascular smooth muscle cells in response to angiotensin II-induced activation of the SHP-2 tyrosine phosphatase. J Cell Physiol. 2005; 205:402–413. [PubMed: 16021628]

50. Levy BD, Bonnans C, Silverman ES, Palmer LJ, Marigowda G, Israel E. Diminished lipoxin biosynthesis in severe asthma. Am J Respir Crit Care Med. 2005; 172:824–830. [PubMed: 15961693]

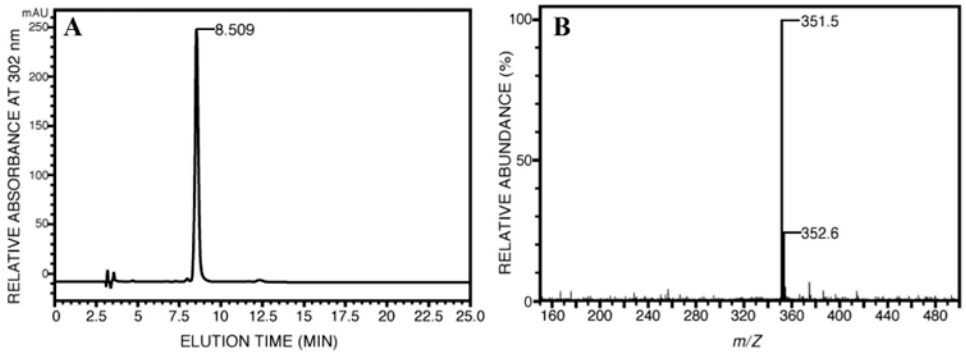

Figure 1.

Quality control analyses of LXA_4. *A*, RP-HPLC of LXA_4 using an Agilent 1100 HPLC with a Vydac C18 RP column (4.6 × 250 mm, 5-μm beads, and 300 Å porosity). Analysis was performed isocratically with methanol/water/acetic acid (65/35/0.1, v/v/v) eluted at 1 ml/min. After 0.6 μg of LXA_4 was injected onto the column, essentially a single major peak eluted at 8.51 min. The collected peak was dried by vacuum centrifugation and then further characterized by MS. *B*, Electrospray ionization-MS of the RP-HPLC major peak using a Waters/Micromass QTOF2 electrospray MS. The sample, dissolved in a 1:1 ratio of water and acetonitrile with 0.1% ammonium hydroxide, was infused into the MS at 10 μl/min. The instrument was operated in the negative ion mode with a source voltage of 3 kV.

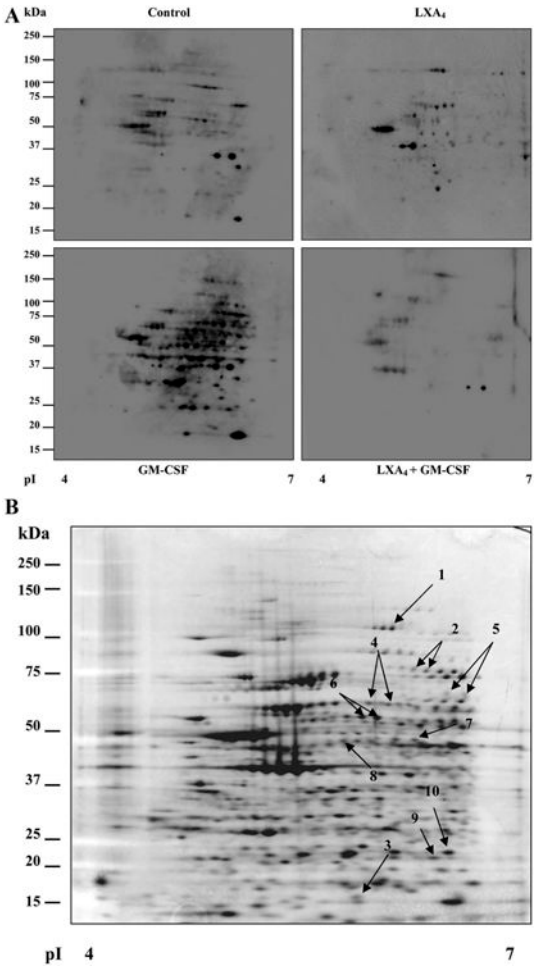

Figure 2.

A, 2DE/LDS-PAGE immunoblot analyses of protein tyrosine phosphorylation from EoL-1 whole-cell lysates (150 μg protein). Samples were focused on 7-cm IPG strips (pH 4–7) and subsequently resolved on 4–16% Tris-LDS polyacrylamide gels and electroblotted onto polyvinylidene difluoride membranes. Protein spots were visualized with anti-pTyr immunostaining. Cell treatments shown were: 1) Control, no treatment; 2) LXA_4 alone (50 nM, 30 min); 3) GM-CSF alone (10 ng/ml, 10 min); and 4) LXA_4 (50 nM, 30 min) followed by GM-CSF (10 ng/ml, 10 min). *B*, Two-dimensional gel of a whole EoL-1 cell lysate stained with Sypro Ruby. After Sypro Ruby staining, gel images were matched with corresponding immunoblots (anti-pTyr stained) and selected spots were subjected to mass analysis by MALD-TOF-TOF mass spectrometry (see Table I for IDs of numbered protein spots). Selected spots were those protein spots whose phosphotyrosine up-regulation was prevented by LXA_4 treatment.

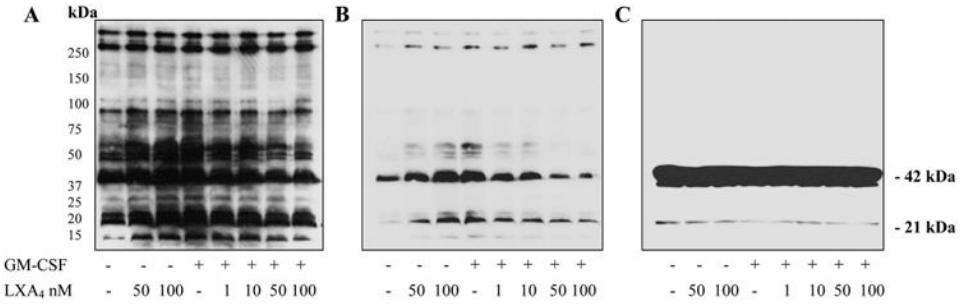

Figure 3.

1DE/LDS-PAGE Western blot analyses of EoL-1 cell lysates from overnight starved cells pretreated for 30 min with increasing concentrations of LXA_4 as shown followed by stimulation with GM-CSF (10 ng/ml, 10 min). *A*, Visualization of protein bands containing phosphotyrosine. Immunoblot analysis with anti-phosphotyrosine staining. *B*, Western blot run under the same conditions as in *A* but with decreased total protein loading for better visualization of intensely stained bands. *C*, Immunoblot was visualized with anti-actin after stripping the anti-pTyr blot shown in *A*.

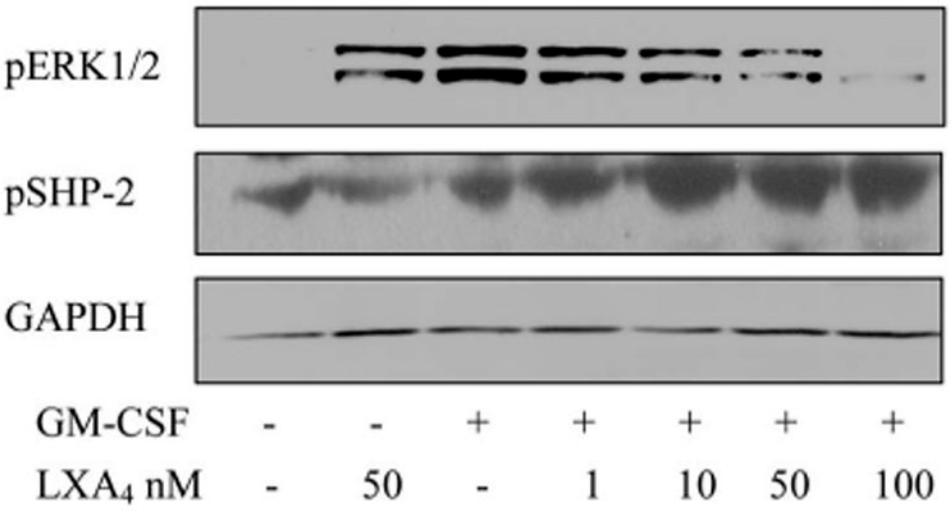

Figure 4.

Western blot analysis of EoL-1 whole-cell lysates pretreated with increasing LXA_4 concentrations as shown followed by 10 min of GM-CSF stimulation (10 ng/ml). The blot was visualized with anti-pERK1/2, anti-pSHP-2, and anti-GAPDH as a sample loading control. The pERK1/2 blot showed inhibition by LXA_4, whereas the pSHP-2 blot showed significant synergistic stimulation by both GM-CSF and LXA_4 together.

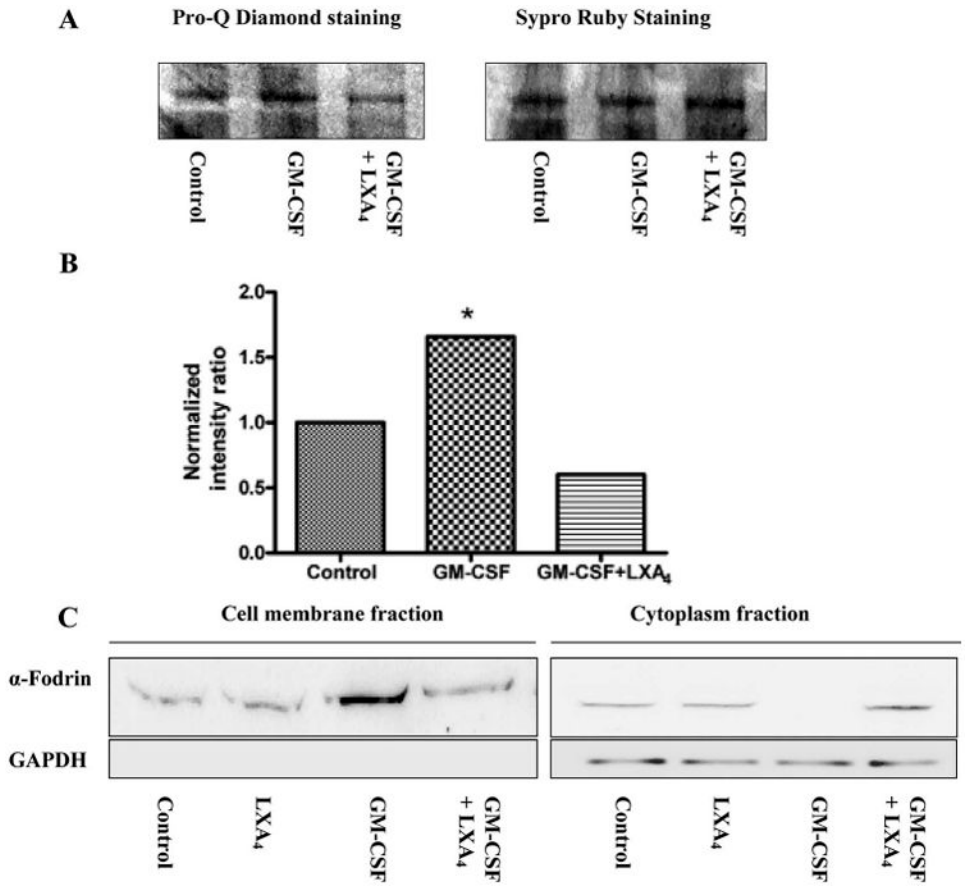

Figure 5.

Effect of LXA_4 on phosphorylation and translocation of α-fodrin induced by GM-CSF. *A*, Fodrin was immunoprecipitated from whole-cell lysates with anti-α-fodrin Abs, and the immunoprecipitate was resolved on one-dimensional 4–16% Tris-LDS polyacrylamide gels and stained as shown. Enhanced phosphorylation of α-fodrin and its inhibition by LXA_4 were observed in immunoprecipitates visualized with the phosphospecific stain Pro-Q Diamond (*left panel*). Equal protein loading was visualized with the Sypro Ruby protein gel stain (*right panel*). *B*, Fluorescent gel scan results of *A* presented as the relative ratio of fluorescence intensity of fodrin phosphorylation after Pro-Q Diamond staining to the fluorescence intensity of the same gel stained with Sypro Ruby, confirming the visual observation in *A* (*, $p < 0.05$, ANOVA using Tukey's posthoc test). *C*, A Triton extraction method was employed to study the cellular distribution of α-fodrin before and after GM-CSF and LXA_4 treatment. Whole EoL-1 cell lysates were fractionated into Triton-soluble (cytoplasmic) and Triton-insoluble (plasma membrane) fractions. Fractions were subjected to Western blot analysis and visualized with anti-α-fodrin immunostaining. The left panel (cell membrane fraction) shows the GM-CSF-induced translocation of fodrin from the cytoplasm to the plasma membrane (*lane 3*), which was inhibited by LXA_4 (*lane 4*). In comparison, the right panel (cytoplasmic fraction) shows the presence of fodrin in the control and LXA_4-treated sample, the absence of fodrin in the GM-CSF-treated sample due to translocation to the plasma membrane (*lane 3*), and the prevention of translocation by LXA_4 (*lane 4*). The lower small panels show the occurrence of the cytoplasmic marker

GAPDH in the cytoplasmic fractions but not the membrane fractions. The observed fodrin translocation was consistent with immunofluorescence results (Fig. 6).

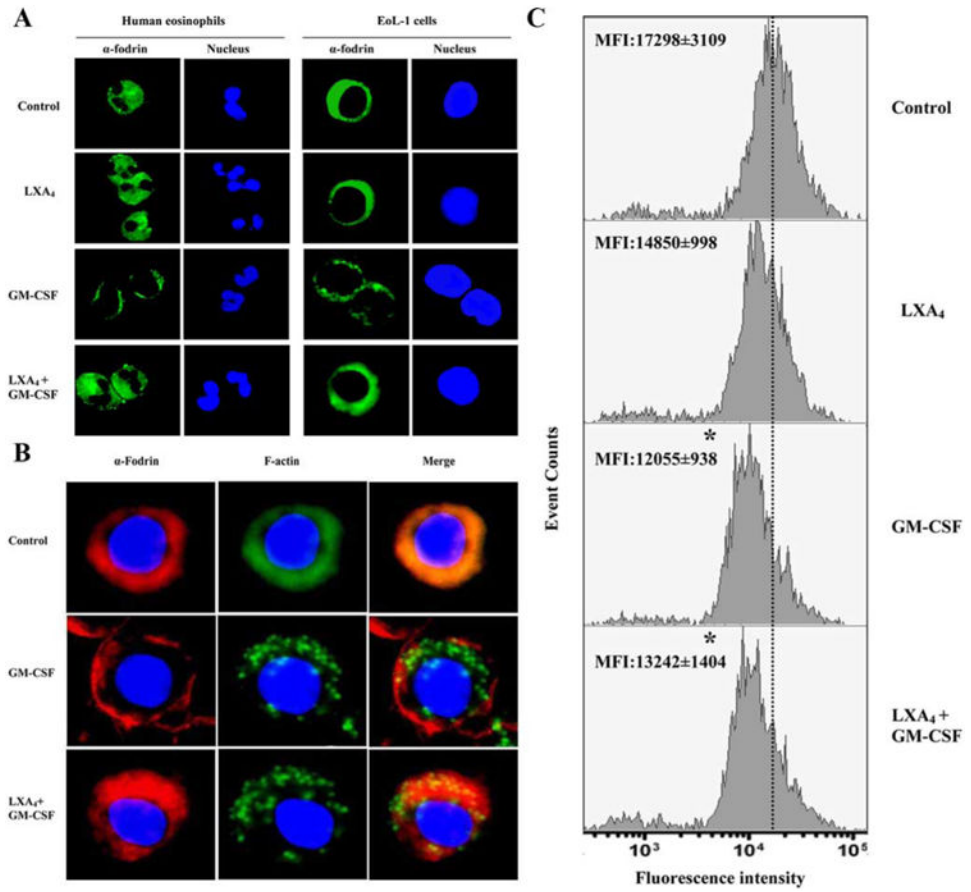

Figure 6.

Subcellular localization of α-fodrin in EoL-1 cells and peripheral blood eosinophils viewed by confocal microscopy. *A*, EoL-1 cells were stained with anti-α-fodrin Ab (*right panel*) (magnification ×128) and human eosinophils were stained with anti-α-fodrin Ab (*left panel*) (magnification ×192); nuclei in both panels were stained with DAPI. *B*, EoL-1 cells were double stained with anti-α-fodrin (rhodamine-labeled secondary Ab) and F-actin-specific FITC-phalloidin. *C*, Flow cytometric analysis of EoL-1 cells stained with FITC-phalloidin for F-actin ($n = 3$; *, $p < 0.05$ when compared with control (ANOVA) using Dunnet's posthoc test).

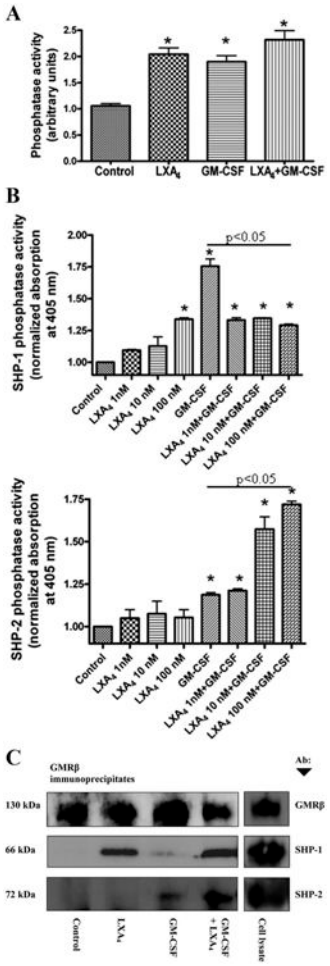

Figure 7.

Total and SHP-1- and SHP-2-associated protein tyrosine phosphatase activity in response to LXA_4 and GM-CSF treatment. *A*, EoL-1 cells were preincubated with 50 nM LXA_4 for 30 min and stimulated with 10 ng/ml GM-CSF for 10 min. Total cellular protein tyrosine phosphatase activity was measured in the whole-cell lysates after free phosphate removal. *B*, Protein tyrosine phosphatase activity of immuno-precipitated SHP-1 (*upper panel*) and SHP-2 (*lower panel*) was measured using a *p*-nitrophenyl phosphate assay. Phosphatase activities are the means ± SEM ($n = 3$). *, $p < 0.05$ when compared with control (ANOVA). *C*, Western blot analysis of GMRβ immunoprecipitates from a cell lysate preparation of 5×10^6 cells per treatment shown: Control, no treatment; LXA_4 alone, 100 nM for 30 min; GM-CSF, 10 ng/ml for 10 min; GM-CSF + LXA_4, pretreatment with 100 nM LXA_4 for 30 min then 10 ng/ml GM-CSF for 10 min; Cell lysate, no treatment. Proteins coprecipitated with anti-GMRβ were visualized on the same blot with specific Abs to SHP-1 and SHP-2. Anti-GMRβ panel confirmed equal protein loading.

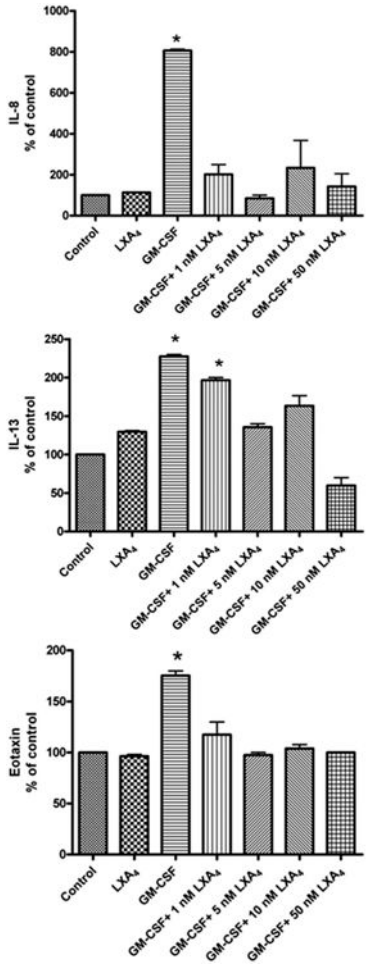

Figure 8.

Effect of LXA_4 treatment on cytokine expression profile. Cytokine secretion was measured in EoL-1 cell supernatants stimulated with GM-CSF (10 ng/ml) after treatment with increasing concentrations of LXA_4 as indicated. Cytokine profiles were measured by Luminex technology after 24 h as described in *Materials and Methods*. Statistical analysis employed ANOVA. *, $p < 0.05$ in comparison with control; results are the means ± SEM of three experiments.

Table I

List of 2DE/MS-identified tyrosine phosphorylated proteins in whole-cell lysates induced by GM-CSF in Eo1-1 cells and inhibited by LXA_4 pretreatment

Spot Position (Fig. 2B) on 2D Gel	Protein ID (Swiss-Prot)	Observed $M_r \times 10^{-3}/pI$	Theoretical $M_r \times 10^{-3}/pI$ (Swiss-Prot)	Peptide Count	Protein Mascot Score	Expectation Value	Accession No. (Swiss-Prot)	Potential Function
1	Glucosidase II *α* subunit	105/5.6	107/5.7	11	161	9.2×10^{-12}	Q14697	Endoplasmic reticulum/stress
2	Ezrin (p81) (cytovillin)	75/5.9	69/5.95	18	274	5.8×10^{-24}	P15311	Membrane/cytoskeletal linkers
3	Profilin-1	15/5.1	15/8.4	5	184	7.9×10^{-14}	P07737	Membrane/cytoskeletal
4	T-complex protein 1 ε subunit	60/5.4	60/5.4	16	108	2.3×10^{-7}	P48643	Chaperone/cytoskeleton regulator
5	Collapsin response mediator protein 2	62/6.0	62/5.9	6	95	4.6×10^{-6}	Q16555	Chaperone/cytoskeleton regulator
6	Protein disulfide-isomerase A3 precursor (p60)	57/5.5	57/5.9	13	157	2.9×10^{-12}	P30101	Chaperone/cytoskeleton regulator
7	Heterogeneous nuclear ribonucleoprotein H	50/5.8	49/5.9	3	69	1.9×10^{-3}	P31943	Metabolic
8	*α*-Fodrin, nonerythroid spectrin *α*-chain	50/5.1	285/5.2	11	66	3.2×10^{-3}	Q13813	Membrane/cytoskeletal linkers
9	Peroxiredoxin-1	25/7.0	28/7.6	3	129	1.8×10^{-9}	P30048	Oxidative stress
10	Protein DJ-1 (oncogene DJ-1)	20/7.0	20/6.33	6	124	5.8×10^{-9}	Q99497	Cell cycle